

## Catalysis by Transition-Metal Carbides. VII. Kinetic and XPS Studies of the Decomposition of Methanol on TiC, TaC, Mo<sub>2</sub>C, WC, and W<sub>2</sub>C

Masahiro ORITA, Isao KOJIMA, and Eizo MIYAZAKI\*

Department of Chemistry, Tokyo Institute of Technology, Ookayama, Meguro-ku, Tokyo 152

(Received July 5, 1985)

The catalytic decomposition of methanol was investigated on a series of powdered transition-metal carbides, such as TiC, TaC, Mo<sub>2</sub>C, WC, and W<sub>2</sub>C, which had been catalytically activated by evacuation at high temperatures. WC was found to produce methyl formate (HCOOCH<sub>3</sub>) with a high selectivity (above 80%), whereas CO and H<sub>2</sub> were mainly produced on clean TaC, Mo<sub>2</sub>C, and W<sub>2</sub>C surfaces. XPS measurements combined with an analysis of the peak intensities revealed that the catalytic activation of WC and TaC was attributable to the removal of surface oxygen and the subsequent formation of monocarbide surfaces. On the other hand, the minor activities leading to the formation of methyl formate on W<sub>2</sub>C and Mo<sub>2</sub>C were concluded to be due to the formation of oxycarbide surfaces. The deuterium distributions in the products during the reaction of CH<sub>3</sub>OD suggest that the methyl formate is produced via the dimerization of the intermediate adspecies, CH<sub>2</sub>O.

The transition metal carbides have been well investigated because of their unique physical properties, such as extremely high melting points, metal-like thermal and electronic conductivities, paramagnetism, and superconductivity.<sup>1)</sup> In addition, they have recently been shown to form an interesting new group of catalysts;<sup>2–7)</sup> the ordered incorporation of carbon atoms into a metal lattice makes chemisorptive and catalytic properties different from those of the parent metals. In order to characterize carbide catalysts, we have investigated the catalytic activities of the carbides of TaC, TiC, WC, and Mo<sub>2</sub>C and have found that they exhibit high activities for the hydrogenation of benzene,<sup>8)</sup> ethylene,<sup>9,10)</sup> and carbon monoxide.<sup>11)</sup> Further, detailed kinetic studies of the hydrogenation of carbon monoxide on powdered WC, W<sub>2</sub>C, and W showed that the catalytic behavior of WC was in contrast with that of W<sub>2</sub>C and W, that is, the activity depended on the carbon/metal ratio and on the lattice structure.<sup>12)</sup>

On the other hand, the dehydrogenation of methanol to produce methyl formate with a high selectivity is currently an important problem in heterogeneous catalysis in relation to C<sub>1</sub> chemistry, and a great deal of research has been conducted into the catalysis of this reaction by metal and metal-oxide surfaces. In a previous paper,<sup>13)</sup> it was found that WC was an excellent catalyst for producing methyl formate from the decomposition of methanol. In the present paper, we wish to report the detailed kinetic and XPS results for TiC, TaC, WC, W<sub>2</sub>C, and Mo<sub>2</sub>C.

### Experimental

Two reaction systems were employed. One was a recirculation reactor, 520 ml in volume, which was directly connected with a gas chromatograph system equipped with two separation columns containing Porapak Q and Molecular sieve 5X. This system also had a U-tube connected to the gas circulation system to remove the condensable products from the reaction system during the

course of the reaction by cooling them to a lower temperature. The other was a UHV batch reactor made of metal and glass. The analysis of the gas-phase composition was done by means of a quadrupole mass analyzer (ANELVA AGA 100). Most of the kinetic measurements were carried out using the former reactor. The distribution of D atoms contained in the products was, however, analyzed by the use of the latter batch reactor.

The reactants, CH<sub>3</sub>OH (obtained from the Nakarai Kagaku Co., 99.6% pure) and CH<sub>3</sub>OD (Merck, 98%), were subjected to vacuum distillation to remove any dissolved air prior to use for the reaction measurements. The powdered catalysts, TiC (99% purity), TaC (99%), WC (99%), W<sub>2</sub>C (99%), and Mo<sub>2</sub>C (99%), were obtained from Furu-uchi Kagaku or M. R. C., and they were catalytically activated as has been described previously<sup>9,10)</sup> by heating in a vacuum at various high temperatures.

The surface analysis of the catalysts was performed on a Hewlett-Packard 5950A ESCA spectrometer, using monochromatic Al K $\alpha$  excited radiation. The samples, pressed into disks, were transferred into the preparation chamber of the spectrometer and subjected to *in situ* heat-treatment in a vacuum.

### Results

**Product Distributions.** Table 1 shows the kinetic results and the product distributions at a 20% conversion of methanol on various carbide catalysts which had been pretreated at high temperatures in a vacuum. As has been reported previously on the hydrogenation of benzene<sup>8)</sup> and ethylene,<sup>9,10)</sup> the catalytic activities for methanol decomposition on TaC and WC were generated by evacuation at 1000 °C for TaC and 700 °C for WC and were almost unchanged up to 1200 °C. TaC produced mainly CO and H<sub>2</sub>, plus a small amount of CO<sub>2</sub>, and the product distribution did not depend on the temperature for the activation of the catalyst, whereas the activity gradually decreased with repeated use. WC produced methyl formate with a high selectivity (above 80%). On the other hand, the catalytic activities of Mo<sub>2</sub>C were found to increase gradually

Table 1. The Kinetic Results and the Product Distributions on Various Carbides

Catalysts	Evacuation temperature	Reaction temperature	Initial rate <sup>a)</sup> of CH <sub>3</sub> OH consumption/(molecule s <sup>-1</sup> g <sup>-1</sup> )	Distribution of carbon-containing products
	°C	°C		%
TiC	1000	300	0	—
TaC	1100	190	$3.1 \times 10^{17}$	CO(91), CO <sub>2</sub> (9)
WC	900	200	$1.5 \times 10^{17}$	HCO <sub>2</sub> CH <sub>3</sub> (81), CO(19)
W <sub>2</sub> C	1200	220	$3.5 \times 10^{17}$	CO(83), HCO <sub>2</sub> CH <sub>3</sub> (17)
Mo <sub>2</sub> C	500	300	$2.2 \times 10^{17}$	CH <sub>4</sub> (84), CO(16)
	800	200	$2.5 \times 10^{17}$	CO(59), HCO <sub>2</sub> CH <sub>3</sub> (41)
	1000	200	$5.0 \times 10^{17}$	CO(100)

a) The initial pressure of methanol is 23 Torr (1 Torr = 133.322 Pa).

with an increase in the evacuation temperature, and the distribution of products also varied with it; following the evacuation at 500 °C, the main products were CH<sub>4</sub>, H<sub>2</sub>O, H<sub>2</sub>, CO<sub>2</sub>, and CO, but at 800 °C they were CO, H<sub>2</sub>, and methyl formate, and at 1000 °C they were only CO, and H<sub>2</sub>. The activities of W<sub>2</sub>C also increased with the increase in the evacuation temperatures, while the product distribution was unchanged. In the table, results at the highest activity are given for W<sub>2</sub>C; the main products were CO, H<sub>2</sub>, and methyl formate, while the selectivity for methyl formate was much lower than that of WC. The activity of TiC was negligible below 300 °C, whereas above 400 °C small amounts of CH<sub>4</sub> and H<sub>2</sub>O were formed.

**Kinetic Measurements.** It is to be noted that, among the metal-carbide catalysts, only WC produced methyl formate with a high selectivity. The detailed kinetic measurements of WC were performed in order to compare the reaction mechanism with the previous results on the transition-metal and oxide catalysts on which the kinetics had already been established. Figure 1 shows the changes in the gas-phase components with the reaction time for the methanol decomposition at 200 °C. It may be seen that in the initial stage of the reaction, methyl formate appeared more rapidly than CO and reached almost a constant concentration after 30 min, while the CO concentration monotonously increased with the time. After 45 min, the U-tube connected to the reactor was cooled to -42 °C to reduce the methanol concentration and to allow the methyl formate to remain in the gas phase. However, the concentration of methyl formate gradually decreased, accompanied by almost twice as large an increase in CO, indicating that the methyl formate decomposed into CO. The selectivity for methyl formate on WC is plotted against the conversion at different reaction temperatures in Fig. 2. With the increase in the reaction temperature the selectivity apparently decreased, however it reaches nearly 100% when the line is extrapolated to zero conversion in each case.

The pressure and temperature dependences were

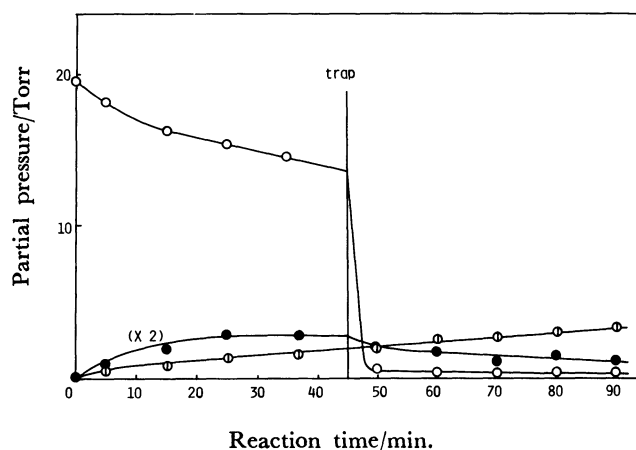


Fig. 1. The change in the gas phase components with the reaction time. After 45 min reaction, the U-tube was cooled down to -42 °C. ○: Methanol, ⊙: carbon monoxide, ●: methyl formate.

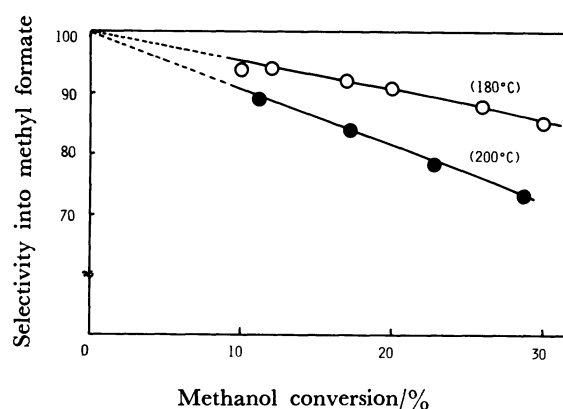


Fig. 2. The selectivity into methyl formate on WC as a function of the methanol conversion. The initial methanol pressure is 21.4 Torr. Reaction temperatures are 180 and 200 °C.

measured by changing the initial pressure of methanol and the reaction temperature respectively. It was found that the plots of the reciprocal of the reaction rate ( $1/r_0$ ) against the reciprocal of the initial pressure ( $1/p_0$ ) gave straight lines for a constant reaction temperatures, as is shown in Fig. 3. The

apparent activation energy was then estimated to be 6.2 kcal<sup>†</sup> mol<sup>-1</sup>. The reaction of CH<sub>3</sub>OD was also investigated using the batch-type reactor. Figure 4 shows the changes in the concentrations of deuterated methyl formate in the gas phase. The line was drawn using the mass peaks of  $m/z=59-64$  and fragment patterns with a least-square approximation;  $d_0$ -methyl formate was predominantly formed in the initial stage of the reaction. The amount of  $d_1$ -species became appreciable with the passage of the time, but the  $d_2$ - to  $d_5$ -species produced by successive exchange reactions were negligible. Furthermore, among the molecules of H<sub>2</sub>, HD, and D<sub>2</sub> produced during the decomposition, HD was predominant at the initial stage of the reaction.

The kinetic measurements were also carried out on Mo<sub>2</sub>C, where the main products were CO and H<sub>2</sub>. A

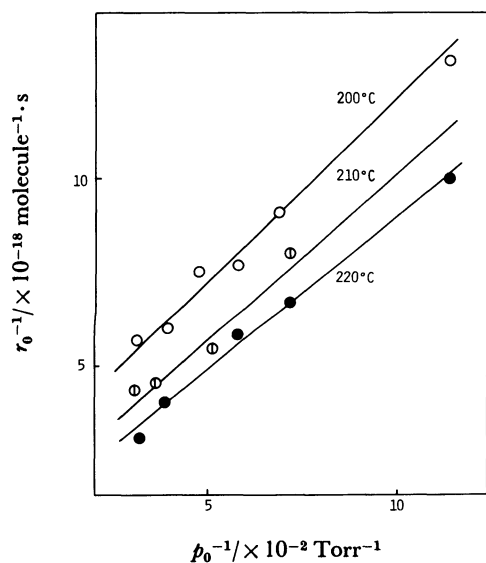


Fig. 3. Plots of the reciprocal of  $\tau_0$  against the reciprocal of  $p_0$ . Reaction temperatures are 200°C, 210°C, and 220°C.

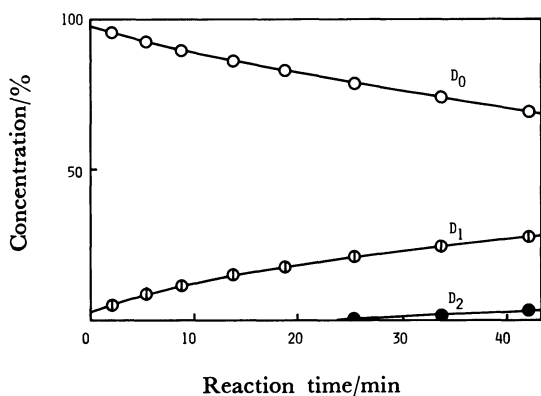


Fig. 4. Changes of concentration of deuterated-methyl formate during the decomposition of CH<sub>3</sub>OD.

<sup>†</sup> 1 cal=4.184 J.

linear relationship similar to that of WC was also obtained between  $1/\tau_0$  and  $1/p_0$ . The reaction order and the apparent activation energy were found to be about 1.0 at 160 °C and 5.4 kcal mol<sup>-1</sup> respectively.

**XPS Measurements.** The XPS spectra were measured for all the catalysts employed. A part of the results have been published previously.<sup>9,10</sup> In Table 2 are summarized the atomic ratios of the surface concentration of the C or O atom to that of metal atoms of the catalysts which had been evacuated under conditions similar to those employed in the kinetic measurements. The ratios of the concentrations of the constituent atoms were estimated from the integrated peak area, upon taking into consideration the photoelectron cross section, the mean free path of electrons, and the apparatus function which is dependent on the kinetic energy of photoelectrons.<sup>14</sup> For the activated WC and TaC surfaces the ratio of C atoms to metals came out to be nearly unity. WC showed no traces of any contaminant oxygen, but TaC was slightly covered with oxygen. The values of the carbon/metal ratio for TiC and W<sub>2</sub>C were lower than in the bulk composition, and their surfaces was found to be covered with oxygen. XPS measurements of Mo<sub>2</sub>C were done for samples evacuated at room temperature, 550, 800, and 1050 °C since the catalytic behavior of Mo<sub>2</sub>C changed with the evacuation temperature. Figure 5 shows the spectra of the Mo 3d, and the O 1s regions for Mo<sub>2</sub>C. Without any heat-treatment, the catalyst surface was mostly covered with oxygen and the Mo 3d states mainly consisted with highly oxidized states, as may be seen in Fig. 5(a) and (e). Following the evacuation at 550 °C, the peaks corresponding to Mo 3d shifted to the lower-binding-energy side, with a mixing of several states. Following the evacuation at 800 °C, two peaks due to the spin-orbit coupling of Mo 3d appeared, along with small shoulders on the higher-binding-energy side. At 1000 °C, they turned into two sharper peaks, and the peak due to O 1s

Table 2. The Atomic Ratio of the Surface Concentration of C or O Atom to that of Total Metallic Species in the Catalysts

	Treatment temperature	Atomic ratio	
		C/M	O/M
TiC	1100 °C	0.8	0.3
TaC	1130	1.1	0.1
WC	1080	0.94	0.0
W <sub>2</sub> C	700 <sup>a)</sup>	0.33	0.3
Mo <sub>2</sub> C	20	0.12	2.9 <sup>b)</sup>
	550	0.15	1.3
	800	0.13	0.8
	1050	0.18	0.1

a) The sample was reduced in the H<sub>2</sub> atmosphere at the temperature. b) Ratio of O to Mo(1) species.

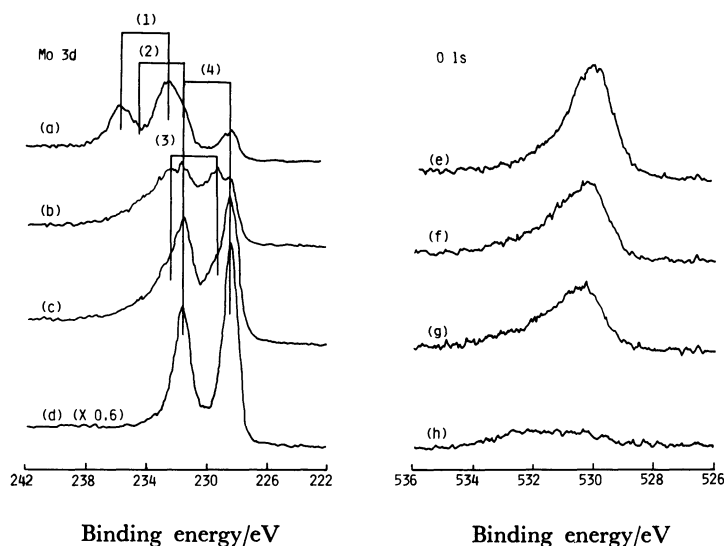


Fig. 5. The change of XPS spectra of Mo 3d and O 1s regions for  $\text{Mo}_2\text{C}$  with pretreated temperatures. (a), (e); 20°C, (b), (f); 550°C, (c), (g); 800°C and (d), (h); 1050 °C.

almost disappeared. The various peaks in the Mo 3d regions described above can be classified into 4 different states, labeled from (1) to (4) in Fig. 5 (a–d). State 1, with the highest binding energy (232.6, 235.6 eV) observed mainly for the untreated surface, can be attributed to the  $\text{Mo}^{6+}$ -oxidized state, since the binding energies are almost identical to the values<sup>15)</sup> reported for  $\text{MoO}_3$  and the observed O/Mo ratio is also close to the ratio of the composition. State 2 (231.5, 234.6 eV) may be assigned to  $\text{Mo}^{5+}$  from the XPS results on the  $\text{Mo}/\text{Al}_2\text{O}_3$  catalyst reported by Patterson et al.<sup>15)</sup> Above the evacuation temperature of 800 °C, State 4 (228.3, 231.5 eV) becomes predominant, and the binding energies are larger than those of Mo metal, suggesting the formation of the carbide.<sup>16)</sup> However, it is noteworthy that the C/Mo ratio is much smaller than that expected from the initial bulk composition. The sample evacuated at 800 °C is also interesting in the sense that it contains a slightly oxidized State 3 (229.4, 232.6 eV); this sample exhibited a special catalytic activity of producing methyl formate.

The XPS spectra of the valence regions are given in Fig. 6. The densities of states below  $E_f$ , which arise mainly from C 2p and metal d-electrons, are distinctive for the carbide catalysts: TiC and TaC have rock salt structure in which the electronic structures can be explained essentially in terms of a simple rigid-band model. The minimum of the density of states occurs at  $E_f$  for TiC; and thus, the extra electrons in Ta are induced to fill the higher-energy antibonding bands to increase the destabilization of TaC. This destabilization effect is compensated for by the lowering of the d-bands relative to the C 2p state for TaC. However, the additional filling of electrons which might occur for VIa-metal

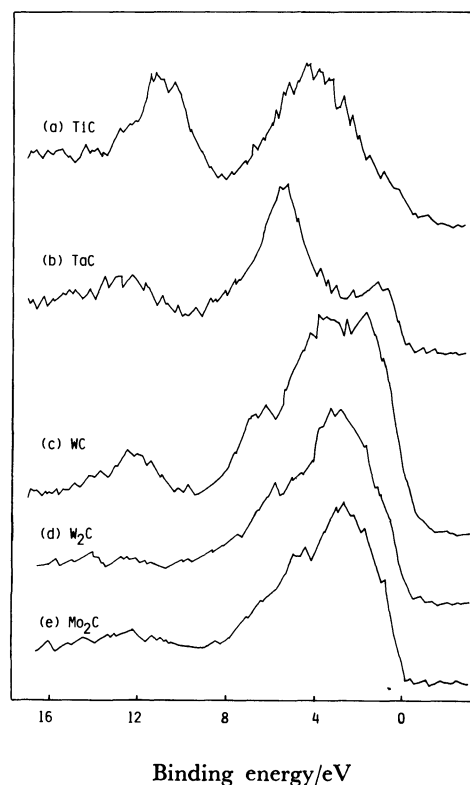


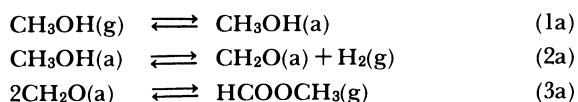
Fig. 6. The XPS valence band spectra of TiC, TaC, WC,  $\text{W}_2\text{C}$ , and  $\text{Mo}_2\text{C}$ .

elements, like W and Mo, change the crystal structure of their carbides into hcp; this results in a more extensive mixing of C 2p with metal d-electrons than in the rock salt structure. The peaks around 12 eV below the  $E_f$  correspond to C 2s bands. The difference in the intensities of the C 2s peaks relative to the density of the states near  $E_f$  is due to the difference in the photoelectron cross-section of d-

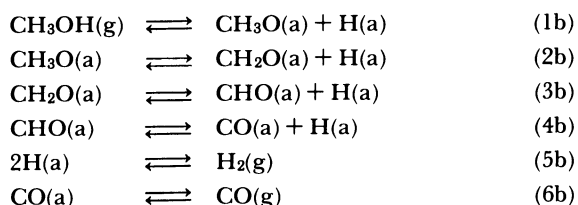
electrons in metal, which increase with an increase in the atomic number.<sup>17)</sup> The present XPS spectra of WC and W<sub>2</sub>C are generally consistent with those reported previously;<sup>18)</sup> it is worth mentioning that the densities of the states of WC near  $E_f$  are higher than those of W<sub>2</sub>C and Mo<sub>2</sub>C. The lower intensities of the C 2s peaks of W<sub>2</sub>C and Mo<sub>2</sub>C, which are about one-half that of WC, suggest the accumulation of metallic species near the surface.

### Discussion

**Reaction Mechanism.** So far, kinetic studies of the decomposition of methanol have been extensively carried out on various transition metals and their oxides.<sup>19–22)</sup> Miyazaki et al. made detailed investigations of Cu<sup>23)</sup> and Ni<sup>24)</sup> catalysts and proposed two different reaction pathways for the decomposition of methanol. A recent review by Joyner also proposed two kinds of reaction mechanisms on the metallic catalysts;<sup>25)</sup> one was a process to form methyl formate as given by Scheme 1, while the other was a process to decompose into CO and H<sub>2</sub> as is given by Scheme 2. The reaction mechanism by Scheme 1 is well known to occur on Cu and Ag catalysts, whereas Scheme 2 is for Pd, Rh, and Ni.



Scheme 1.



Scheme 2.

The present results of methanol decomposition on the transition metal carbide catalysts may be interpreted within a similar framework; WC was found to produce methyl formate with a high selectivity, whereas the other carbides produced mainly CO and H<sub>2</sub>. The one slight exception is on TiC and Mo<sub>2</sub>C, where CH<sub>4</sub> and H<sub>2</sub>O were produced. Since these products were generally formed on metal oxide catalysts<sup>26)</sup> and since the XPS spectra showed presence of considerable oxygen on the catalysts, this distribution may safely be attributed to the oxide formation on the surfaces. The high selectivity for methyl formate on WC makes it easy to investigate the reaction mechanism. The linear relationship in

Fig. 3 leads to the following rate equation in the initial stage of the reaction on WC

$$r_0 = a p_0 / (1 + b p_0), \quad (1)$$

where  $a$  and  $b$  are constants. This rate Eq. 1 suggests that the decomposition of the adsorbed methanol into an intermediate adsorbate is the rate-determining step. As is shown in Fig. 4, the selective formation of  $d_0$ -methyl formate and HD from CH<sub>3</sub>OD in the initial stage of the reaction strongly suggests that the reaction given by Step (2a) proceeds on the surface. These findings are quite similar to those observed on the Cu surface.<sup>23)</sup>

Scheme 2 shows, on the other hand, that the decomposition into CO and H<sub>2</sub> is initiated by the dissociative adsorption of methanol into methoxide and H species. As no methyl formate was detected, the intermediate methoxide is considered to decompose directly via Steps (2b)–(4b) into CO. Further, the UPS results of NbC(111)<sup>27)</sup> revealed the formation of methoxide after the admission of methanol, suggesting the involvement of a surface reaction like Step (2b) on W<sub>2</sub>C, TaC, and clean Mo<sub>2</sub>C, where the main products are carbon monoxide and hydrogen. The similar pressure dependence of the rate on Mo<sub>2</sub>C to the rate equation (1) suggests that Step (2b) in Scheme 2 is the rate-determining step. Thus, the reaction Schemes (1 and 2) given above are also effective for the metal-carbide catalysts; the different product distributions among the carbide catalysts seem to result from the different stabilizations of intermediate species, CH<sub>3</sub>O(a) and CH<sub>2</sub>O(a).

**Characteristics of Transition-Metal Carbides.** (i) In the previous studies, the surface oxygen was found to play a dominant role in the catalytic activation of transition-metal carbides; the presence of oxygen strongly reduced the activity of the hydrogenation of benzene<sup>9)</sup> and ethylene<sup>9,10)</sup> on TaC. The present kinetic and XPS measurements also indicate that the removal of surface oxygen is necessary for the generation of the activity of methanol decomposition on TaC and WC. On the other hand, Mo<sub>2</sub>C pretreated in vacuo at 800 °C yielded activities comparable to those of TaC and WC, even though its XPS spectra revealed the presence of a large amount of oxygen on the surface. Interestingly, on such a surface with oxygen, an appreciable amount of methyl formate is formed, whereas clean Mo<sub>2</sub>C evacuated at 1100 °C, produced merely CO and H<sub>2</sub>. This shows that the surface oxygen on Mo<sub>2</sub>C forms an oxycarbide<sup>3)</sup> like MoO<sub>x</sub>C<sub>y</sub> and that its electronic states are varied to be suitable for stabilizing the CH<sub>2</sub>O(a) adsorbate. The minor selectivity into methyl formate observed on W<sub>2</sub>C may also be ascribed to the partial formation of oxycarbide. Thus, such oxycarbide–oxygen in dimetallic carbides of Mo<sub>2</sub>C, and W<sub>2</sub>C apparently

behaves as "carbon" in the corresponding monocarbides, though MoC has not been obtained as a stable substance.

(ii) It is generally accepted that the electronic states near  $E_f$  have great importance for the chemical activity of a surface. Information about these states is available from the measurements using photoelectron spectroscopy. The few studies<sup>18,28,29)</sup> which have been done following the first suggestion by Levy and Boudart<sup>30)</sup> that the catalytic activity of WC is to be attributed to the density of states similar to Pt conflict as to the point whether or not the chemical activity can be directly related to the state densities of the valence regions. As is shown in Fig. 6, it seems to be sure that the onset of sharp peaks at  $E_f$  of TaC is responsible for the appearance of larger catalytic activity as compared with TiC and that the catalytic properties of WC can be related to the higher state density at  $E_f$  than at  $W_2C$ , although it is not clear in all cases that the higher density at  $E_f$  is related to the higher catalytic activity.

(iii) In the present work, the distinctive selectivity between WC and  $W_2C$  for methyl formate was shown. The improvement of selectivity for methyl formate by alloying into carbides was also reported by Ko et al.,<sup>4,5)</sup> TPRS studies on Mo and W single crystals have shown that methyl formate is not formed from formaldehyde on the pure metal surfaces, but is apparently formed after the carburization of these crystals. Similar results were also obtained on powdered Ni catalysts at the reaction temperature of 30–80 °C.<sup>31)</sup> The formation of carbide may result in the reduction of the chemical activity of the adsorbing gases and in suppression of the complete decomposition into C, O, and H atoms which occurs on the original pure metals.

(iv) It is likely that, for alloy systems with rigid crystal structures, like metal carbides, the surface arrangement of the constituent atoms plays a dominant role in the catalytic activity. According to recent calculations of the band structures of the bulk and surface of WC<sup>32)</sup> by Mattheiss and Hamann, the metal-terminated  $W(1\times 1)$  surface of WC(0001) exhibits a distinctive surface-state density due to d-electrons at  $E_f$ . The work function of the metal-terminated surface is also much smaller than that of the carbon-terminated surface. Recently, surface spectroscopic studies of transition-metal carbides have been performed under uhv conditions using such single-crystal surfaces as TiC(100), TiC(111),<sup>33,34)</sup> NbC(100), and NbC(111).<sup>27)</sup> An important finding of these studies is that their cleaned (111) surfaces consist of metals on the topmost layer; thus they are chemically more active than the (100) surfaces which consist of a regular array of coexisting metal and carbon atoms. The previous comparative investigation of WC,  $W_2C$ , and W powdered catalysts for the hydrogenation of CO also showed that the catalytic

behavior of WC is quite in contrast with those of  $W_2C$  and W; the metal-terminated surfaces are responsible for the catalysis, since the electronic states of the topmost metal layer of WC(0001) would preferably be modified by the second carbon underlayer to produce an active site for the hydrogenation of carbon monoxide, while, on the other hand, the influence of the third carbon layer on the topmost tungsten layer of  $W_2C$  would be small. These effects may contribute to the distinctive selectivity between WC and  $W_2C$  presently observed for the formation of methyl formate. Therefore, the complete carburization of W to form WC seems necessary for the appearance of a new catalytic feature to produce methyl formate on WC.

## References

- 1) L. E. Toth, "Transition Metal Carbides and Nitrides," Academic Press, New York/London (1971).
- 2) S. T. Oyama and G. L. Haller, *Catalysis*, **3**, 333 (1982).
- 3) M. Boudart, S. T. Oyama, and L. Leclercq, "Proceeding of 7th Intern. Congr. Catalysis, Tokyo, 1980," Kodansha, Tokyo (1981), p. 578.
- 4) E. I. Ko and R. J. Madix, *Surf. Sci.*, **112**, 373 (1981).
- 5) E. I. Ko, J. B. Benziger, and R. J. Madix, *J. Catal.*, **64**, 132 (1980).
- 6) P. N. Ross, Jr., and P. Stonheart, *J. Catal.*, **39**, 298 (1975).
- 7) P. N. Ross, Jr., and P. Stonheart, *J. Catal.*, **48**, 42 (1977).
- 8) E. Miyazaki and K. Fuse, *Nippon Kagaku Kaishi*, **1972**, 815.
- 9) I. Kojima, E. Miyazaki, Y. Inoue, and I. Yasumori, *J. Catal.*, **59**, 472 (1979).
- 10) I. Kojima, E. Miyazaki, Y. Inoue, and I. Yasumori, *J. Catal.*, **73**, 128 (1982).
- 11) I. Kojima, E. Miyazaki, and I. Yasumori, *J. Chem. Soc., Chem. Commun.*, **1980**, 573.
- 12) I. Kojima, E. Miyazaki, Y. Inoue, and I. Yasumori, *Bull. Chem. Soc. Jpn.*, **58**, 611 (1985).
- 13) E. Miyazaki, I. Kojima, and M. Orita, *J. Chem. Soc. Chem., Commun.*, **1985**, 108.
- 14) M. Uda and K. Maeda, *Kinzoku Butsuri Seminar*, **3**, 11 (1975).
- 15) T. A. Patterson, J. C. Carver, P. E. Leyden, and D. M. Hercules, *J. Phys. Chem.*, **80**, 1700 (1976).
- 16) Yu. M. Shul'ga, A. P. Borisov, V. D. Makhaev, and A. P. Borisov, *J. Organomet. Chem.*, **164**, 47 (1979).
- 17) J. H. Scofield, *J. Electron Spectro. Relat. Phenom.*, **8**, 129 (1976).
- 18) R. J. Colton, J.-T. J. Huang, and W. Rabalis, *Chem. Phys. Lett.*, **34**, 337 (1975).
- 19) B. A. Sexton, *Surf. Sci.*, **88**, 299 (1979).
- 20) S. R. Bare, J. A. Strocio, and W. Ho, *Surf. Sci.*, **140**, 415 (1984).
- 21) R. Ryberg, *J. Chem. Phys.*, **82**, 567 (1985).
- 22) W. Hirshwald and D. Hofmann, *Surf. Sci.*, **140**, 415 (1984).
- 23) E. Miyazaki and I. Yasumori, *Bull. Chem. Soc. Jpn.*, **40**, 2012 (1967).
- 24) I. Yasumori, T. Nakamura, and E. Miyazaki, *Bull.*

- Chem. Soc. Jpn.*, **40**, 1372 (1967).
- 25) R. W. Joyner, *Catalysis*, **5**, 19 (1981).
- 26) F. Nozaki, *Hyomen(Surface)*, **21**, 194 (1983).
- 27) I. Kojima, M. Orita, and E. Miyazaki, *Surf. Sci.*, **160**, 153, (1985).
- 28) L. H. Bennett, J. R. Curthill, A. J. McAlister, N. E. Erickson, and R. E. Watson, *Science*, **184**, 563 (1973).
- 29) J. E. Houston, G. E. Laramore, and R. L. Park, *Science*, **185**, 258 (1974).
- 30) R. B. Levy and M. Boudart, *Science*, **181**, 547 (1973).
- 31) E. Miyazaki, *Proc. VIth Intern. Congr. on Catalysis*, **1**, 408 (1976).
- 32) L. F. Mattheiss and D. R. Hamann, *Phys. Rev. B* **30**, 1731 (1984).
- 33) C. Oshima, M. Aono, S. Zaiman, Y. Shibata, and S. Kawai, *J. Less- Common. Metals*, **82**, 69 (1981).
- 34) A. M. Bradshaw, J. F. van der Veen, F. J. Himpsel, and D. E. Eastman, *Solid State Commun.*, **37**, 37 (1980).
-